Analyst

ROYAL SOCIETY OF CHEMISTRY

PAPER

View Article Online
View Journal

Check for updates

Cite this: DOI: 10.1039/c9an02289a

An FcεRI-IgE-based genetically encoded microfluidic cell sensor for fast Gram-negative bacterial screening in food samples†

Hui Jiang,[a,b] Jun Yang,[b] Donglei Jiang[c] and Xiulan Sun *[a]

Received 14th November 2019,
Accepted 9th January 2020

DOI: 10.1039/c9an02289a

rsc.li/analyst

An FcεRI-IgE-based genetically encoded microfluidic cell sensor was constructed for fast Gram-negative bacterial screening in food samples. CD14-Fcε IgE, produced by the gene engineered antibodies (GEAs) technology, was used for the recognition of the target bacteria or lipopolysaccharide (LPS). Stable cell lines expressing GCaMP6s, a genetically encoded indicator of calcium flux, were first established for monitoring mast cell activation and improving detection sensitivity. The microfluidic system was designed to improve automation and control the reaction time. Once Gram-negative bacteria bound to the CD14-Fcε IgE on the RBL-2H3 cell surface, RBL-2H3 cell receptor (FcεRI)-induced Ca^{2+} signaling pathway was immediately activated to release Ca^{2+}. The elevated intracellular Ca^{2+} triggers GCaMP6s for reporting the presence of Gram-negative bacteria. The developed biosensor was able to detect 80 CFU mL^{-1} Gram-negative bacteria within 2.5 min in pure culture samples. The biosensor was used to detect Gram-negative bacteria in pork samples. With its short screening time and easy operation, the proposed biosensor shows promise in future applications of foodborne pathogen testing in 1 h to 1 day.

Introduction

In recent years, adaptability of bacteria has increased their drug resistance. New, reproducible and evolved foodborne bacteria are increasing rapidly,[1] making people unprepared for sudden outbreaks of foodborne diseases. Bacterial contamination has affected human health, economic development and social stability, so rapid and accurate methods to detect low concentrations of target bacteria are required to assess food safety within hours to a day.[2,3] Traditional culturing methods, which are the gold standard, are time-consuming and labor-intensive,[4] taking up to 3–7 days to obtain negative results and longer time for the confirmation of positive results.[3] Immunology[5,6] detection methods are sometimes less sensitive. Even though these assays based on genotype[7,8] are highly sensitive and specific, the extended analysis time is sometimes inconvenient. In addition, immunology- and genotype-based methods can only detect known bacteria, which leads to the omission of unknown bacteria. Most important of all, since most of our test samples in food inspection are going to be negative, it would be wise to use screening techniques that can exclude negative samples very quickly, preferably within hours. Efforts could therefore be made to identify pathogens in positive samples, which may require lengthy analysis to provide results in a few days.[3] Recently, a strategic approach involving a rapid, two-step, high-throughput screening to rule out negatives followed by a confirmatory test that could accomplish product testing in 1 h to 1 day was put forward by Bhunia.[3] The early fast identification and initial non-targeted screening of bacterial contamination is vital to food safety, manpower saving and improvement of efficiency in inspection organization. For the above reasons, it is urgent to establish a rapid, labor-saving, and sensitive analysis approach for the non-targeted screening of bacterial contamination.

A cell-based biosensor (CBB) is an analytical device that uses living cells as sensitive elements to detect the functional information of cells and properties of objects through signal conversion.[2] Living cells are extremely sensitive to modulations or disturbances in "normal" physiological microenvironment. Therefore, CBBs are employed to screen and monitor "external" or environmental agents capable of causing perturbations of living cells.[9,10] The first microbe- or cell-based sensor was developed by Divies.[11] Since the early works by Rechnitz and

[a]State Key Laboratory of Food Science and Technology, School of Food Science and Technology, National Engineering Research Center for Functional Food, Synergetic Innovation Center of Food Safety and Nutrition, Jiangnan University, Wuxi, Jiangsu 214122, China. E-mail: sxlzyz@jiangnan.edu.cn
[b]Nanjing Institute for Food and Drug Control, Nanjing, Jiangsu 211198, PR China
[c]College of Food Science and Engineering, Nanjing University of Finance and Economics, Collaborative Innovation Center for Modern Grain Circulation and Safety, Key Laboratory of Grains and Oils Quality Control and Processing, Nanjing, Jiangsu 210023, PR China

†Electronic supplementary information (ESI) available. See DOI: 10.1039/c9an02289a

Published on 18 January 2020. Downloaded by University of Liverpool on 2/13/2020 6:38:21 AM.

Published on 18 January 2020. Downloaded by University of Liverpool on 2/13/2020 6:38:21 AM.

coworkers during the 1980s,[12,13] numerous examples of combinations of a variety of cell species with various transducer devices or systems have been demonstrated. Giaever *et al.* reported an electrical mammalian cell biosensor that can continuously track morphological changes of adherent cells, providing quantitative data from both sparse and confluent cultures.[14] Rider *et al.* reported the first cell sensor that used B lymphocytes to recognize specific bacteria with the help of membrane-bound IgM antibodies.[15] CBBs have been rapidly developed over the past decade. The CBB, as an analytical tool for detecting bacteria, pesticide residues, toxins and other harmful substances in food, has aroused extensive interest.[2] Throughout the new generation of biosensors, cell receptors are directly or indirectly used in the first step of biological recognition, and then ligand-binding-induced secondary cellular responses are detected.[16] Therefore, receptors are crucial in the construction of cell-based biosensors. CD14 is a synergistic protein for TLR4 to recognize ligand LPS and can be used as a high-affinity receptor for Gram-negative bacteria to identify and bind to Gram-negative bacterial virulence factor LPS, but it does not have a signal transmission function.[17] Fc receptor is the C-terminal receptor of the Fc fragment, which presents on the surface of B cells, mast cells, killer cells, macrophages and other immune cells. Mast cells are usually used in the construction of biosensors because they can be activated dramatically after exposure to antigen within a few minutes.[18,19] Signals transformed by biosensors can be further recorded and quantified. FcεRI on the surface of RBL-2H3 mast cell line can bind immunoglobulin E (IgE) so that subsequent encounters with antigens will cross-link the FcεRI-IgE complex.[20] This triggers cellular degranulation[21] and the release of chemicals, for example intracellular calcium,[22] reactive oxygen species[23] and β-hexosaminidase.[24]

The calcium flux occurs earlier and can be monitored *via* calcium fluorescent indicators. There have been a few studies on calcium kinetics after the stimulation of living cells since the technique limits the determination of cytoplasmic calcium using calcium-sensitive dyes. To overcome some of the limitations of calcium-sensitive dyes, a genetically encoded calcium indicator (GECI) was produced. GCaMP, as a commonly used GFP-based GECI, is the product of the fusion of a single green fluorescent protein (GFP), calmodulin (CaM) and the M13 fragment of the myosin light chain kinase in smooth muscle cells.[25] When calcium binds to CaM, the conformation changes to surround the M13 peptide, and its hinge area binds to M13. Ca^{2+}-CaM-M13 interaction leads to the environment change of the EGFP chromogenic groups and promotes an obvious increase of fluorescence intensity.[26] GCaMP has undergone several upgrades to optimize sensitivity and kinetics.[26,27] The new generation of GCaMPs, such as GCaMP6s, 6m, and 6f, offers significant improvements in brightness and dynamic range.[28] GCaMP6s is widely used to detect small changes in calcium due to its higher sensitivity and brighter fluorescence.[29,30] Moreover, a CBB with GCaMPs can be used without any calcium-sensitive dye regent in the process of detection, which greatly reduces the test cost.

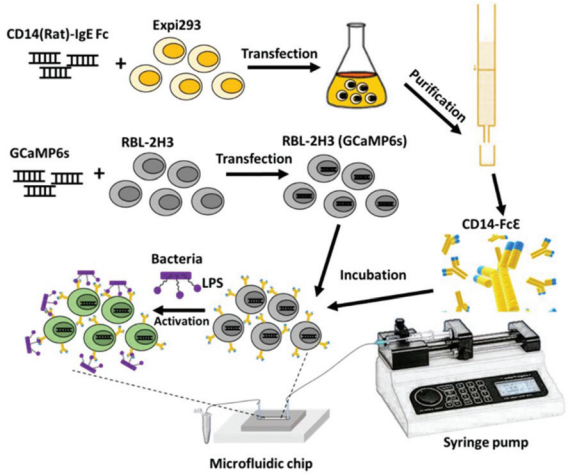

Scheme 1 Schematic illustration of the preparation and the working principle of the biosensor.

In this paper, RBL-2H3 mast cell (co-incubated with CD14-Fcε) is used to identify and detect Gram-negative bacteria or LPS. Scheme 1 presents the preparation and working principle of the biosensor. Stable calcium indicating cell lines were constructed by the transfection of GCaMP6s into RBL-2H3 mast cells. CD14-Fcε combines with the FcεRI receptor on the surface of the RBL-2H3 mast cell. When the target bacteria or LPS cross-links the adjacent CD14-Fcε/FcεRI complexes, FcεRI receptors come together, causing a succession of accumulation and phosphorylation of intracellular signaling molecules,[31] leading to the rapid influx of extracellular Ca^{2+} into the cytoplasm and the release of proinflammatory factors (such as histamine and β-hexosaminidase). During this process, the influx of Ca^{2+} occurs within seconds, and the change of $[Ca^{2+}]_{cyto}$ is relatively obvious. After binding to Ca^{2+}, the green fluorescence can be observed in the RBL-2H3 cells transfected with GCaMP6s. The fluorescence intensity, which indicates the presence of the Gram-negative bacteria or LPS, is proportional to $[Ca^{2+}]_{cyto}$. Combining the high sensitivity of GCaMP6s to Ca^{2+}, the rapid response of RBL-2H3 mast cells (co-incubated with CD14-Fcε) to Gram-negative bacteria or LPS and the miniaturization and automation of the microfluidic system, an FcεRI-IgE-based genetically encoded microfluidic cell sensor was designed for Gram-negative bacteria or LPS detection to rule out negative samples rapidly.

Experimental

Reagents

α-MEM was purchased from HyClone Lab Inc. Fetal bovine serum, pGH vector, pcDNA3.1 vector and anti-His tag antibody were purchased from Life Technologies. A23187 and trypsin solution were obtained from Sigma Aldrich. All bacteria culture media were obtained from Sinopharm Chemical Reagent Co., Ltd. Endotoxin-free Plasmid Maxiprep Kit was

 This journal is © The Royal Society of Chemistry 2020

Published on 18 January 2020. Downloaded by University of Liverpool on 2/13/2020 6:38:21 AM.

purchased from Qiagen. HBSS, Ca^{2+} and Mg^{2+}-free HBSS, MTT, BCA protein assay kit and goat anti-mouse IgG-HRP were obtained from Beyotime Biotechnology (Nantong, China). Enhanced chemiluminescence reagent (ECL) was obtained from Millipore. NuPAGE Bis-Tris Gels and nitrocellulose membrane were purchased from Invitrogen. Goat anti-mouse IgG-FITC and anti-CD14 antibody were obtained from Santa Cruz Biotechnology. Lentiviral vectors pLenti-CMV-GCaMP6(s)-2A-Tdtomato lentiviral vector and polybrene were purchased from Obio Technology (Shanghai) Corp., Ltd.

Cell lines

RBL-2H3 cells were purchased from the Cell Bank of Type Culture Collection of Chinese Academy of Sciences (Shanghai, China). The RBL-2H3 mast cells were maintained in α-MEM with 15% (v/v) FBS, 100 U mL^{-1} penicillin, and 100 U mL^{-1} streptomycin in a humidified atmosphere of 95% air and 5% CO_2 at 37 °C. In this study, P1–P10 cells were used for the biosensor development. CD14-Fcε was expressed by Expi293 cells (Thermo Scientific), which were suspended cultured in Expi293 Expression Medium (Thermo Scientific) in a humidified Multitron incubator shaker at 37 °C with 8% CO_2.

Bacterial strains

Escherichia coli ATCC 25922, *Salmonella enterica serovar Typhimurium* ATCC 14028 and *Shigella dysenteriae* ATCC 13313 were obtained from Zhangjiagang Customs District P.R. China. *Listeria monocytogenes* ATCC 19115 and *Bacillus cereus* CMCC (B) 63303 were obtained from the Nanjing Institute for Food and Drug Control. All strains were cultured overnight and centrifuged for collection. The bacterial pellets were resuspended in HBSS and centrifuged for collection.

Construction, expression and purification of recombinant chimeric protein

The recombinant antibody was named CD14-Fcε. The target protein sequence of the monocyte differentiation antigen CD14 precursor [*Rattus norvegicus*] was obtained from the NCBI protein database (Accession: NP_068512). The target protein sequence of the CH3 and CH4 domains of *Rattus norvegicus* IgE were obtained from the UniPro proteomic database (UniProtKB-P01855). The sequence of the CH3ε and CH4ε domains were fused downstream of CD14 linked by a (G4S)3 linker.[32,33] To facilitate the purification, we inserted a His-tag after the C-terminal of CD14. The chimeric sequence was synthesized by Detai Biotechnology (Nanjing, China) and cloned into pGH. After being confirmed by DNA sequencing, the target gene was cloned into pcDNA3.1, and then transformed into the *E. coli* DH5α to prepare the transfection-grade plasmid CD14(Rat)-IgE Fc.

The preparation process of recombinant chimeric protein is shown in Scheme 1. CD14(Rat)-IgE Fc plasmids were transfected into Expi293 cells by calcium phosphate precipitation. The culture supernatant with the secreted recombinant chimeric IgE was collected after 6 days, and was filter-sterilized by using a membrane filter (0.22 μm pore size), and was dialyzed against 25 mM Tris, 150 mM NaCl (pH 8.0), and then purified using a Ni^{2+} affinity chromatography column as follows: the supernatants were diluted with an equal volume of binding buffer (20 mM Na_2HPO_4/NaH_2PO_4, 0.5 M NaCl, pH 7.4), and applied onto the column at a flow rate of about 1 mL min^{-1}. In the end, the chimeric protein was eluted by increasing the imidazole concentrations at a flow rate of 1 mL min^{-1}. The protein was dialysed overnight at 4 °C to remove the imidazole. The purified CD14-Fcε can be stored at −80 °C for more than one year after packaging.

Identification and biological properties of the chimeric protein

The purified protein was confirmed by SDS-PAGE and western blotting. After electrophoresis, the gel was stained with Coomassie Brilliant Blue R-250. Besides, the purified proteins were transferred from the gel to the nitrocellulose membrane (NCM) using an iBlot®2 Dry Blotting System (Invitrogen). Next, nitrocellulose membranes were incubated in 5% BSA for 2 h. Blots were incubated in mouse anti-His tag antibody at 4 °C overnight. Then the blot was incubated with goat anti-mouse IgG-HRP for 1.5 h. Target proteins were detected by an enhanced chemiluminescence (ECL) substrate and scanned with a FluorChem FC3 camera system (ProteinSimple).

Immunofluorescence was used to analyze whether purified CD14-Fcε could identify the target analysts. Either 1×10^7 CFU mL^{-1} *E. coli* (G^-) or *S. aureus* (G^+) was incubated with the 6 μg mL^{-1} CD14-Fcε. After washing, the bacteria were incubated with 2 g mL^{-1} anti-CD14 mAb and goat anti-mouse IgG-FITC in turn.

Scanning electron microscopy (SEM) imaging

RBL-2H3 mast cells were mixed with *E. coli* for 10 min and then processed as follows for SEM imaging. The sample was fixed in 3% paraformaldehyde at 4 °C overnight, and then post-fixed in 1% osmium tetroxide at 4 °C for 1 h. The samples were then dehydrated using 30, 50, 70, 85, 95, and 100% graded ethanol for 15–20 min each. The sample was then subjected to critical point drying and coated with gold-palladium. the as-prepared sample could be observed by SEM (Hitachi model S-4800).

Fabrication of the microfluidic chip

The microfluidic chip (Wenhao Chip Tech., China) consisted of two parts: a polydimethylsiloxane (PDMS) channel layer and a glass sheet. The PDMS channel layer was made by photolithography and replica-molding, and then it was bonded to the glass sheet. The PDMS channel was 40 μm in height, 1000 μm in width and 2 cm in length. Two blunt needles were inserted into each end of the microfluidic channel (Fig. 1). The cell suspension or bacterial suspension was injected by a syringe pump. The microfluidic channel outlet was connected to a waste recycling tube. The microfluidic chip is reusable and should be sterilized before each use.

Published on 18 January 2020. Downloaded by University of Liverpool on 2/13/2020 6:38:21 AM.

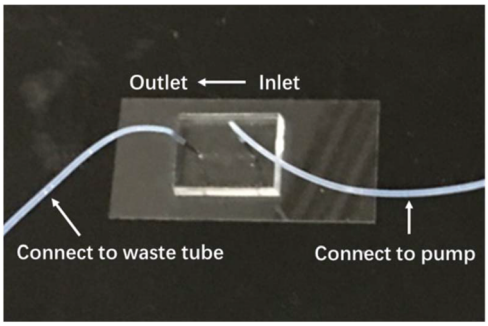

Fig. 1 Microfluidic chip.

Preparation of the biosensor

The RBL-2H3 mast cells were transfected with the Ca^{2+}-indicator GCaMP6s, namely lentiviral vector pLenti-CMV-GCaMP6(s)-2A-Tdtomato. RBL-2H3 mast cells were seeded into 24-well plates 24 hours before transduction, 5×10^4 cells per well. The lentiviral vector was added onto each well at an MOI of 10, 20, 40 and 60 with 6 μg mL^{-1} polybrene for 4 hours. Seventy-two hours post transduction with DNA containing lentiviral vectors, transduction efficiency and cell sorting were determined by assaying for red fluorescent protein (tdTomato) expression. FACS analysis was performed on the BD Biosciences-FACS Aria III cell sorter using CellQuest Pro software for analysis. The cell lines can be stored in a liquid nitrogen tank for 5–10 years or more in theory. If GCaMP6s is found missing, positive cell lines can be screened by flow cytometry again.

In order to study the response of RBL-2H3 mast cells mediated by CD14-Fcε IgE and verify the ability of the constructed biosensor to recognize Gram-negative bacteria and LPS, changes of cell fluorescence intensity were used to analyze the degree of cellular response to Gram-negative bacterial or LPS stimulation. The whole process of detecting Gram-negative bacteria or LPS by the biosensor was observed and analyzed by CLSM. The selected stably transfected RBL-2H3 mast cells were inoculated into the self-made microfluidic chip at 37 °C for confocal laser scanning microscopy (CLSM) (Carl Zeiss) observation. After the cells were adhered to the wall, they were washed by HBSS. CD14-Fcε (1 μg mL^{-1}) was co-incubated with stably transfected RBL-2H3 mast cells for 1 h at 37 °C, and the cells were washed. Upon adding different concentrations of Gram-negative bacteria or LPS using a syringe pump, fluorescence was immediately observed and determined by CLSM. In time-dependent assays, fluorescence images of stimulated cells were taken every 0.5 s and recorded continuously for 5 min. F_t is the EGFP fluorescence value at any point in time, and F_0 is the stable baseline of EGFP fluorescence produced by $[Ca^{2+}]_{cyto}$ before Gram-negative bacteria or LPS addition. F_t/F_0 against time curve was used to quantify EGFP fluorescence changes with time. In dose-dependent assays, response produced by $[Ca^{2+}]_{cyto}$ is presented as relative fluorescence intensity. We defined relative fluorescence intensity as the ratio between EGFP fluorescence of the treated cells and background fluorescence of the untreated cells.

Preparation of real samples

Fresh pork bought from the supermarket was contaminated with different kinds of bacteria to mimic bacterial contamination. Twenty-five grams of fresh pork and 225 mL HBSS were mixed in a filtra bag and beaten with a paddle homogenizer for 1–2 min. The filtrate was collected. To obtain fresh pork samples contaminated with bacteria at 10^2 CFU mL^{-1}, 1 mL 10^3 CFU mL^{-1} *E. coli* ATCC 25922, *S. dysenteriae* ATCC 13313, *S. Typhimurium* ATCC 14028, *L. monocytogenes* ATCC 19115 or *B. cereus* CMCC(B) 63303 was respectively added to 9 mL of the filtrate.

Results and discussion

Preparation of CD14-Fcε

Engineering chimeric IgE was successfully used in mast cell biosensors by combining the antigen-binding domain with the Fc domain of the IgE molecule.[20] The CH3 and CH4 domains are the smallest fragments of full-length IgE that can bind to FcεRI and pre-sensitize RBL-2H3 cells.[33,34] Based on this, a chimeric IgE which contained the Fc domain of the IgE molecule and CD14(Rat) was constructed.

Plasmid construction. As shown in Fig. S1,† the protein amino acid sequence of CD14-Fcε IgE was optimized by the MaxCodon™ Optimization Program (V13). A full-length splice primer was designed and a clone plasmid containing the target gene was constructed (Fig. S2A†). The target gene was then subcloned into the pcDNA3.1 vector and transformed into *E. coli* DH5α to prepare the transfected plasmid. Agarose gel analysis was performed on the extracted plasmid. Fig. S2B† shows that the obtained plasmid meets the requirements of transfection grade plasmid, which can be used for the next transfection operation.

Protein purification. The expression of target secreted recombinant chimeric IgE was analyzed by SDS-PAGE. As shown in Fig. S3A,† CD14-Fcε is expressed. Through Ni-IDA affinity chromatography, the target protein is mainly found in the eluting component Lane 3–6 (Fig. S3B†). The results of protein purity analysis are shown in Fig. S3C.† There is no obvious heteroband on the electrophoretic chart, so the purity of the target protein after purification is relatively high (>90%). The specificity of target protein was analyzed by western blotting with an anti-His tag antibody. The purified protein was quantified by BCA (Fig. S4†). The concentration of the sample was 0.599 mg mL^{-1}. As shown in Fig. S5,† CD14-Fcε bound to Gram-negative bacteria, indicating successful preparation of the target chimeric antibody.

Construction of the biosensor

Lentiviral transfection and stable cell line screening. The plasmid profile of pLenti-CMV-GCaMP6(s)-2A-Tdtomato is shown in Fig. S6.† As shown in Fig. S7,† the transfection

 This journal is © The Royal Society of Chemistry 2020

Published on 18 January 2020. Downloaded by University of Liverpool on 2/13/2020 6:38:21 AM.

efficiencies of MOI = 10, 20, 40 and 60 are 61.0%, 73.2%, 81.6% and 92.3%, respectively. Therefore, lentivirus was transfected with MOI = 60 and the stably transfected cell lines were obtained by flow cytometry.

Stability of the transfected cell lines. In order to study the activity and genetic stability of the transfected cells, the cells were passed on continuously for 6 weeks. As shown in Fig. S8,† the results show that the percentage of viable cell and fluorescence efficiency does not change significantly, indicating better cell activity and genetic stability.

Cell fluorescence test. To test whether stably transfected cell lines can fluoresce through the production of intracellular Ca^{2+}, we used A23187 to stimulate cells to produce Ca^{2+} signals. As a carrier of Ca^{2+}, A23187 can lead to the rapid entry of extracellular Ca^{2+} into the cells, thus causing Ca^{2+} signal to be generated inside the cells. It can be seen from Fig. S9† that GCaMPs can be activated by the Ca^{2+} signal in the cytoplasm of RBL 2H3 and make cells fluoresce. With the increase of A23187 concentration, $[Ca^{2+}]_{cyto}$ increases, and the fluorescence intensity of cells increases. It was demonstrated that the established stably transfected RBL-2H3 cell model could be used for the detection of Ca^{2+} in the cytoplasm. At present, GCaMPs have been widely used in the changes of calcium ions in nerve cells,[35,36] but there are a few reports on the application in other cells (such as epithelial cells, immune cells, *etc.*).[30,37] It is suggested from this study that GCaMPs can be used for monitoring $[Ca^{2+}]_{cyto}$ changes in RBL-2H3 cells, providing a flexible new tool for the study of calcium signaling in immune cells.

Establishment of mast cell detection model

In order to verify whether the as-constructed biosensor can be used for the detection of specific antigen, *E. coli* ATCC 25922 and chimeric IgE protein CD14-Fcε were used to determine the function of RBL-2H3 cells. *E. coli* was used as the model bacteria in this paper, since it is one of the most common pathogens causing foodborne diseases.

CD14 can be used as the receptor of Gram-negative bacteria and can recognize and bind to Gram-negative bacterial virulence factor LPS. Therefore, Gram-negative *E. coli* ATCC 25922 was selected as the representative strain containing LPS. The binding of *E. coli* ATCC 25922 to the RBL-2H3 cells (P1–P10) incubated with CD14-Fcε was observed by SEM (Fig. 2).

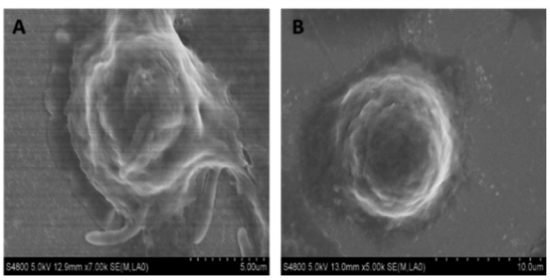

Fig. 2 SEM images of *E. coli* ATCC 25922 and RBL-2H3 cell (A) and RBL-2H3 cell (B).

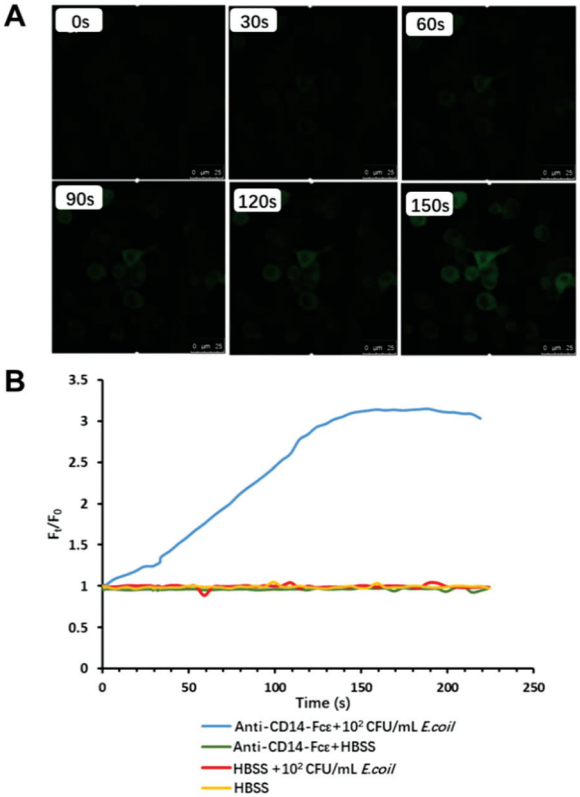

Fig. 3 Response of RBL-2H3 cells (co-incubated with CD14-Fcε) exposed to 10^2 CFU mL^{-1} *E. coli* ATCC 25922. (A) Time lapse imaging. (B) Fluorescence curve.

As shown in Fig. 3A, RBL-2H3 cells incubated with CD14-Fcε were able to specifically identify *E. coli* ATCC 25922 and activate the signal transduction pathways in the cells, leading to fluorescence. The cells rapidly produced fluorescence after being activated. F_t/F_0 *versus* time was monitored using a CLSM. With exposure of 10^2 CFU mL^{-1} *E. coli* ATCC 25922, the fluorescence intensity gradually increased with the extension of time from 0 s, and reached the maximum fluorescence intensity within 2.5 min, and then gradually flattened (Fig. 3A and B). Fig. 3B showed an obvious increase of the F_t/F_0 value after stimulation with *E. coli* ATCC 25922 when compared to the control (without antigen or without antibody), which confirmed the sensing principle. The results show that the constructed RBL-2H3 cell senor can be used for the detection of Gram-negative bacteria with good specificity and short detection time (within 2.5 min).

Detection in pure culture

The biosensor was used to detect *E. coli* ATCC 25922 in pure culture with the concentration ranging from 10^1 to 10^5 CFU mL^{-1}. The control group was HBSS without *E. coli* ATCC 25922. When the concentration of *E. coli* ATCC 25922 varied within the range of 10^2–10^5 CFU mL^{-1}, there is a significant difference in relative fluorescence intensity in comparison with the control group ($*p < 0.05$, $**p < 0.01$, $n = 3$). As shown

Published on 18 January 2020. Downloaded by University of Liverpool on 2/13/2020 6:38:21 AM.

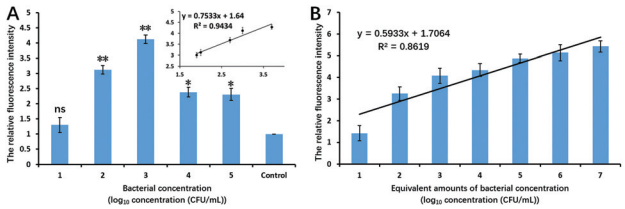

Fig. 4 Detection of *E. coli* ATCC 25922. (A) Correlation between the relative fluorescence intensity and bacteria concentration. Insert: calibration curve, the concentration ranging from 8×10^1 CFU mL^{-1} to 5×10^3 CFU mL^{-1}. (* and ** represent statistical significance among groups, $*p < 0.05$, $**p < 0.01$, $n = 3$). (B) Correlation between the relative fluorescence intensity and LPS extracted from *E. coli* ATCC 25922, which is equal to a bacterial concentration of 10^1 CFU mL^{-1} to 10^7 CFU mL^{-1}.

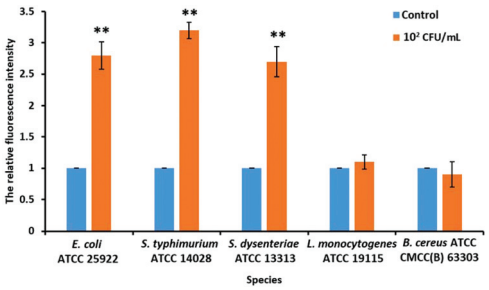

Fig. 5 Detection of bacteria in pork samples. Plot of the biosensor's response to different kinds of bacteria in pork. (* and ** represent statistical significance among groups, $*p < 0.05$, $**p < 0.01$, $n = 3$).

in Fig. 4A, there is a clear linear positive correlation between the relative fluorescence intensity and bacterial concentration from 8×10^1 CFU mL^{-1} to 5×10^3 CFU mL^{-1}. The equation was $y = 0.7533x + 1.64$ ($R^2 = 0.9434$), where y is the relative fluorescence intensity and x is $\log_{10}$ concentration (CFU mL^{-1}). It is observed that the relative fluorescence intensity dropped at 10^4 CFU mL^{-1} and 10^5 CFU mL^{-1} *E. coli* ATCC 25922. However, as shown in Fig. S10,† there is a linear positive correlation between the release rate of β-hexosaminidase and bacterial concentration from 10^1 to 10^7 CFU mL^{-1}. These results apparently do not agree with the previous fluorescence detection results. This may be because the high concentrations of *E. coli* ATCC 25922 in the solution block the observations of the fluorescent signal of RBL-2H3 cells. However, this does not affect the ability of the biosensor to detect low concentrations of bacteria, and the release rate of β-hexosaminidase tests verifies the correctness of the fluorescence detection results at low concentrations of bacteria stimulation. Fig. 4A shows that the biosensor can detect 10^2 CFU mL^{-1} *E. coli* ATCC 25922 within 2.5 min. The fluorescence intensity increased at 10^1 CFU mL^{-1} *E. coli* ATCC 25922, but was not found to be significantly different compared to the control ($^{ns}p > 0.05$, $n = 3$). Therefore, the LOD of *E. coli* ATCC 25922 was 80 CFU mL^{-1} (S/N = 3). All of the experiments were conducted three times under the same conditions. For comparison purposes, we summarized some recently reported methods for bacteria detection in Table S1.† Non-targeted screening for bacterial contamination is the highlight of this study. The currently developed method has also shown superiority over the other methods in terms of rapidity, sensitivity and ease of use.

When equivalent amounts of extracted LPS (10^1–10^7 CFU mL^{-1}) were used to stimulate the biosensor, the relative fluorescence intensity was positively correlated with the amount of LPS (Fig. 4B). The linear regression equation was expressed as $y = 0.5933x + 1.7064$ ($R^2 = 0.8619$), where y is the relative fluorescence intensity, and x refers to the equivalent amounts of bacterial concentration ($\log_{10}$ (CFU mL^{-1})).

Detection in real sample

The biosensor was further evaluated with bacteria inoculated pork extract samples to study the application of the biosensor. According to the pure culture experiments, we selected 10^2 CFU mL^{-1} *E. coli* ATCC 25922, *S. dysenteriae* ATCC 13313, *S. typhimurium* ATCC 14028, *L. monocytogenes* ATCC 19115 and *B. cereus* CMCC(B) 63303 for the test.

The biosensor's response to real sample showed a similar response to the pure culture. As shown in Fig. 5, there are significant differences between control and real samples inoculated with 10^2 CFU mL^{-1} *E. coli* ATCC 25922, *S. dysenteriae* ATCC 13313 or *S. typhimurium* ATCC 14028 ($**p < 0.01$, $n = 3$). It is worth noting that there was a difference in the relative fluorescence intensity between detection in real sample and detection in pure culture with 10^2 CFU mL^{-1} *E. coli* ATCC 25922, but the results were not statistically significant. This may be because the food composition in the pork sample affects the specific adsorption of bacteria on the surface of RBL-2H3 cells, resulting in the decreased sensitivity of the biosensor. However, this does not affect the detection of the target object by the biosensor. Fluorescence signal was not detected when Gram-positive bacteria *L. monocytogenes* ATCC 19115 or *B. cereus* CMCC(B) 63303 was added, demonstrating the specificity of this sensing system for Gram-negative bacteria and not Gram-positive bacteria potentially found in food samples. To sum up, this study proves that the developed biosensor can be used for the rapid screening of Gram-negative bacteria.

Conclusions

Herein, an FcεRI-IgE-based genetically encoded microfluidic cell sensor was successfully constructed and used to screen Gram-negative bacteria. *E. coli* ATCC 25922 can be quantified in the 8×10^1 CFU mL^{-1} to 5×10^3 CFU mL^{-1} concentration range, with an LOD of 80 CFU mL^{-1} in pure culture within 2.5 min. The method was successfully used to detect *E. coli* ATCC 25922, *S. dysenteriae* ATCC 13313 and *S. typhimurium* ATCC 14028 in pork samples, which verified the ability of the method for real samples analysis. This proposed method can be directly used to fast-screen Gram-negative bacterial in food samples without the need for cultivation of bacteria, and thus has more practical value for application. The cost of one test is

 This journal is © The Royal Society of Chemistry 2020

Published on 18 January 2020. Downloaded by University of Liverpool on 2/13/2020 6:38:21 AM.

usually about $0.70 (passage numbers of cells before 10, including the cost of cell culture).

The novelty of this study is the construction of immune cell lines (RBL-2H3 mast cell lines) stably expressing GCaMP6s, which are preserved in our laboratory. This has never been reported before. This design provides a new idea for the construction of immune cell sensor based on Ca^{2+} signal pathway. The developed mast cell lines have a wide application prospect, since rapid detection of other targets can also be easily realized by preparing various kinds of target IgE antibodies that bind to FcεRI on the RBL-2H3 cell surface. The combination of stably transfected RBL-2H3 mast cells and a self-made microfluidic chip lays the foundation for designing an FcεRI-IgE-based genetically encoded microfluidic cell sensor with easy operation and fast screening to accomplish food-borne pathogens testing in 1 h to 1 day.

Conflicts of interest

There are no conflicts to declare.

Acknowledgements

This work has been supported by National Key Research and Development Program of China (2017YFC0211303), National Natural Science Foundation of China (31601535), Natural Science Foundation of Jiangsu Province (BK20180160, BK20190584), Science and Technology Development Project of Nanjing (201716006), Special Program of the State Administration for Market Regulation (2019YJ047), Research Project of Jiangsu Food and Drug Administration (20170210), Science and Technology Program of Nanjing Administration for Market Regulation (Kj2019042), Open Project Program of State Key Laboratory of Dairy Biotechnology (SKLDB2019-005).

Notes and references

1 M. Askar, M. Faber, C. Frank, H. Bernard, A. Gilsdorf, A. Fruth, R. Prager, M. Höhle, T. Süß and M. Wadl, *Euro Surveill*, 2011, **16**, 19883.
2 Y. Ye, H. Guo and X. Sun, *Biosens. Bioelectron.*, 2019, **126**, 389–404.
3 A. K. Bhunia, *Future Microbiol.*, 2014, **9**, 935–946.
4 E. Grilli, R. Bari, A. Piva, T. S. Edrington, D. W. Pitta, W. E. Pinchak, D. J. Nisbet and T. R. Callaway, *Foodborne Pathog. Dis.*, 2015, **12**, 56–61.
5 R. Chen, X. Huang, J. Li, S. Shan, W. Lai and Y. Xiong, *Anal. Chim. Acta*, 2016, **947**, 50–57.
6 Q. Guo, J.-J. Han, S. Shan, D.-F. Liu, S. S. Wu, Y.-H. Xiong and W.-H. Lai, *Biosens. Bioelectron.*, 2016, **86**, 990–995.
7 S. V. Angus, S. Cho, D. K. Harshman, J.-Y. Song and J.-Y. Yoon, *Biosens. Bioelectron.*, 2015, **74**, 360–368.
8 W. H. Chin, Y. Sun, J. Hogberg, T. L. Quyen, P. Engelsmann, A. Wolff and D. D. Bang, *Mol. Cell. Probes*, 2017, **32**, 24–32.
9 D. A. Stenger, G. W. Gross, E. W. Keefer, K. M. Shaffer, J. D. Andreadis, W. Ma and J. J. Pancrazio, *Trends Biotechnol.*, 2001, **19**, 304–309.
10 C. Ziegler, *Fresenius' J. Anal. Chem.*, 2000, **366**, 552–559.
11 C. Divies, *Ann. Microbiol.*, 1975, **126**, 175–186.
12 C. A. Corcoran and G. A. Rechnitz, *Trends Biotechnol.*, 1985, **3**, 92–96.
13 G. Rechnitz and M. Ho, *J. Biotechnol.*, 1990, **15**, 201–217.
14 I. Giaever and C. R. Keese, *Nature*, 1993, **366**, 591–592.
15 T. H. Rider, *Science*, 2003, **301**, 213–215.
16 S. Subrahmanyam, S. A. Piletsky and A. P. F. Turner, *Anal. Chem.*, 2002, **74**, 3942–3951.
17 S. D. Wright, R. A. Ramos, P. S. Tobias, R. J. Ulevitch and J. C. Mathison, *Science*, 1990, **249**, 1431–1433.
18 D. Jiang, P. Zhu, H. Jiang, J. Ji, X. Sun, W. Gu and G. Zhang, *Biosens. Bioelectron.*, 2015, **70**, 482–490.
19 W. Xin, W. Yao, X. Gao, Z. You, S. Gao, L. Kang, Q. Li, Y. Zhou, H. Yang, P. Jiang and J. Wang, *J. Biomed. Nanotechnol.*, 2014, **10**, 3318–3328.
20 T. Curtis, R. M. Z. G. Naal, C. Batt, J. Tabb and D. Holowka, *Biosens. Bioelectron.*, 2008, **23**, 1024–1031.
21 R. M. Williams and W. W. Webb, *J. Cell Sci.*, 2000, **113**, 3839–3850.
22 B. Moreau, S. Straube, R. J. Fisher, J. W. Putney and A. B. Parekh, *J. Biol. Chem.*, 2005, **280**, 8776–8783.
23 Y. Suzuki, T. Yoshimaru, T. Matsui, T. Inoue, O. Niide, S. Nunomura and C. Ra, *J. Immunol.*, 2003, **171**, 6119–6127.
24 K. Brockow, *Hautarzt*, 2013, **64**, 102–106.
25 P. M. Bayley, W. A. Findlay and S. R. Martin, *Protein Sci.*, 1996, **5**, 1215–1228.
26 J. Akerboom, J. D. V. Rivera, M. M. R. Guilbe, E. C. A. Malave, H. H. Hernandez, L. Tian, S. A. Hires, J. S. Marvin, L. L. Looger and E. R. Schreiter, *J. Biol. Chem.*, 2009, **284**, 6455–6464.
27 Y. Shindo, A. Fujimoto, K. Hotta, K. Suzuki and K. Oka, *J. Neurosci. Res.*, 2010, **88**, 3125–3132.
28 M. Ohkura, T. Sasaki, J. Sadakari, K. Gengyo-Ando, Y. Kagawa-Nagamura, C. Kobayashi, Y. Ikegaya and J. Nakai, *PLoS One*, 2012, **7**, e51286.
29 D. Boehning, R. L. Patterson, L. Sedaghat, N. O. Glebova, T. Kurosaki and S. H. Snyder, *Nat. Cell Biol.*, 2003, **5**, 1051–1061.
30 M. I. Garcia, J. J. Chen and D. Boehning, *Cell Calcium*, 2017, **61**, 44–49.
31 D. MacGlashan Jr., *Curr. Opin. Immunol.*, 2008, **20**, 717–723.
32 L. Hellman, U. Pettersson, A. Engstrom, T. Karlsson and H. Bennich, *Nucleic Acids Res.*, 1982, **10**, 6041–6049.
33 M. Basu, J. Hakimi, E. Dharm, J. A. Kondas, W. H. Tsien, R. S. Pilson, P. Lin, A. Gilfillan, P. Haring, E. H. Braswell, M. Y. Nettleton and J. P. Kochan, *J. Biol. Chem.*, 1993, **268**, 13118–13127.
34 M. Qu, B. M. Boruah, W. Zhang, Y. Li, W. Liu, Y. Bi, G. F. Gao, R. Yang, D. Liu and B. Gao, *Biosens. Bioelectron.*, 2013, **43**, 412–418.

35 A. Muto, M. Ohkura, T. Kotani, S.-I. Higashijima, J. Nakai and K. Kawakami, *Proc. Natl. Acad. Sci. U. S. A.*, 2011, **108**, 5425–5430.

36 J. Akerboom, T.-W. Chen, T. J. Wardill, L. Tian, J. S. Marvin, S. Mutlu, N. C. Calderon, F. Esposti, B. G. Borghuis, X. R. Sun, A. Gordus, M. B. Orger, R. Portugues, F. Engert, J. J. Macklin, A. Filosa, A. Aggarwal, R. A. Kerr, R. Takagi, S. Kracun, E. Shigetomi, B. S. Khakh, H. Baier, L. Lagnado, S. S. H. Wang, C. I. Bargmann, B. E. Kimmel, V. Jayaraman, K. Svoboda, D. S. Kim, E. R. Schreiter and L. L. Looger, *J. Neurosci.*, 2012, **32**, 13819–13840.

37 B. Cai, X. Chen, F. Liu, J. Li, L. Gu, J. R. Liu and J. Liu, *Assay Drug Dev. Technol.*, 2014, **12**, 342–351.

Published on 18 January 2020. Downloaded by University of Liverpool on 2/13/2020 6:38:21 AM.

 This journal is © The Royal Society of Chemistry 2020